Proceedings of the 36th International Conference on Ocean, Offshore & Arctic Engineering
OMAE2017
June 25-30, 2017, Trondheim, Norway

OMAE2017-61390

THEORETICAL AND EXPERIMENTAL STUDY OF HEADING STABILITY AND HEADING CONTROL OF A TURRET-MOORED FPSO

Karl E. Kaasen
SINTEF Ocean[1]
Trondheim, Norway

Halgeir Ludvigsen
SINTEF Ocean[1]
Trondheim, Norway

Ivar Nygaard
SINTEF Ocean[1]
Trondheim, Norway

Kristian Aas
Statoil
Oslo, Norway

ABSTRACT

The behaviour and characteristics of a turret-moored FPSO subjected to loading from waves, wind and current are investigated. Of particular importance is to find out if fishtailing instabilities may occur, and if such instability can be disclosed by simple criteria involving basic parameters of the system's mathematical model. Eight cases from model tests are chosen for theoretical study and time domain simulation. Four of the cases involve heading control with thrusters.

For the stability study, a simplified linear model in sway and yaw is formulated. It is shown that the inherent characteristics of the model depend on the strengths and relative directions of the metocean processes. The eigenvalues of the sway-yaw model are computed for the eight selected cases to check the stability. A simple approximate criterion for heading stability is derived from the sway-yaw model. It is assumed, but not proven, that the criterion is a sufficiency criterion for stability.

Both the experiments and the simulations show that the eight cases are stable. This is also confirmed by the eigenvalues of the sway-yaw model, while the simple criterion wrongly deems several cases unstable. The simple stability criterion is therefore probably conservative, at least when there is significant damping in the system. In one additional hypothetical case with only wave excitation and weak or lacking stability, the simplified criterion agrees well with the model test and simulation.

Heading control is necessary when a heading different from the natural weathervaning heading is wanted. The controller used in the experiments and simulations is of simple SISO PID type. With control, the heading variations are reduced significantly.

INTRODUCTION

For station-keeping of an FPSO (Floating Production Storage and Offloading) vessel, spread mooring or turret mooring are the most common choices and have their respective advantages and disadvantages, which depend on a number of factors, see discussion in [1]. The most notable difference between these two systems is that the heading of a spread-moored ship is fixed, while turret mooring allows the ship to rotate about the turret, either by the aid of thrusters, or naturally by weathervaning. Thus, the loading from the metocean environment can be kept at a minimum. There also exists a modified type of spread mooring, the DICAS concept, where the restraint on the heading is lesser than for ordinary spread mooring, thereby allowing heading adjustment in a limited sector [12].

A turret-moored vessel needs heading control if the heading, as determined by the vessel's weathervaning properties, is not acceptable for operational or safety reasons, e.g.:

- The natural weathervaning heading is not good enough with regard to environmental loading.
- It is necessary to direct the bow against the waves to minimize rolling of consideration for the comfort of the crew or the conditions for the on board processing plant.
- It is necessary to reduce vessel motions during offloading to a shuttle tanker.
- Should a gas leak occur, it must be possible to rotate the FPSO such that the wind does not carry the gas cloud towards the living quarters.

[1] Formerly MARINTEK. SINTEF Ocean from January 1st 2017 through an internal merger in the SINTEF group.

- The turret-moored FPSO becomes dynamically unstable without control.

A turret-moored ship may experience instability in the sense that the static equilibrium position and heading are not stable. For a stable ship, the motion will be variations about the mean position and heading. In calculations, the mean position and heading can usually be represented by the hypothetical static equilibrium, which is calculated with the static environmental loads acting, i.e. the mean loads from current, wind and waves that act when the vessel is still. For a certain position and heading, the static environmental loads counterbalance the force and moment from the mooring system, which is the definition of static equilibrium.

The equilibrium heading is that for which the mean environmental moment about the centre of the turret is zero. The resultant environmental load on the ship depends on the equilibrium heading. The load is usually not minimum for the equilibrium heading. The magnitude of the equilibrium offset depends on the stiffness of the mooring system.

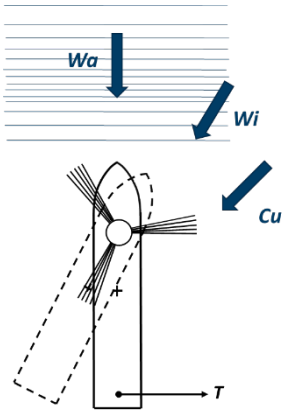

Figure 1 Keeping bow against waves using thruster. Dashed contour indicates the natural weathervaning orientation. *T* is force from thruster.

A necessary condition for a stable equilibrium heading is: If the ship is rotated a small angle about the turret centre from an angle of equilibrium, the static environmental loads must create an opposing moment. In other words, there must be a resistance against departing from the equilibrium. If, when the weather changes, the heading changes automatically from one stable equilibrium to another the vessel has the weathervaning property. If any combination of current, wind and waves results in some stable equilibrium, the vessel is absolutely weathervaning stable

For an unstable ship and mooring, an initial deviation from the equilibrium will self-amplify, and the vessel will enter into a state of slow, stationary oscillation in the horizontal plane. This oscillation is known as fishtailing. The phenomenon is governed by nonlinear interaction between sway and yaw. Sometimes a ship may be conditionally stable or conditionally weather-vaning, these properties depending on the environmental condition.

In addition to motions caused by fishtailing instability, there will be motion generated by the random variations in the loading from wind and waves. For cases of major instability, the stochastic dynamic loading may have the appearance of random fluctuations on top of large fishtailing oscillations. If the fishtailing instability is moderate, it may not be discernible through the random loading. When fishtailing happens, heading control is necessary to quench it.

In the following, we study the conditions for heading stability based a simplified linear sway-yaw model for the turret-moored FPSO. We compare the stability results with time domain simulations using a detailed nonlinear model with six degrees of freedom of motion, and with results from model tests.

The FPSO

The object of study is a turret moored FPSO which is being designed for a prospective field in the Barents Sea, see Figure 2. In the process of design, a number of FPSO candidates have emerged, differing in size and arrangement. The FPSO under study represents one of the candidates, and not necessarily the final FPSO.

Figure 2 The studied FPSO

Table 1 shows some main particulars of the FPSO. The turret centre is located 71 m forward of midship, which corresponds to 26 % of L_{pp}. Note that the radius of gyration in yaw is greater in the ballasted condition than in the loaded condition. In spite of smaller displacement, the yaw inertia is therefore greater for the ballasted ship.

The mooring system consists of 15 lines arranged in three bundles with 120˚ symmetry (Figure 3). The lines are identical and composed of an upper wire rope segment and a lower chain segment. The water depth is 373 m. The pretension is the same for all lines and is 2066 kN in the loaded state and 2209 kN in the ballasted state.

The thruster system consists of three identical azimuth thrusters located as one group aft. The thrusters have a rated power of 3.5 MW each, which corresponds to a maximum thrust of 553 kN. The thruster system is not needed for relief of the mooring lines during storms, since the mooring system is designed to have

sufficient capacity to survive ULS weather conditions with required safety factors.

Table 1 Main particulars of the FPSO.

Item	Ballasted	Loaded
Length between perpendiculars, L_{pp}	274 m	
Breadth moulded, B	54.8 m	
Depth moulded	30.0 m	
Distance from AP to turret centre	208 m	
Draft, T	17. 1 m	21.3 m
Displacement, Δ	215600 t	275900 t
Radius of gyration in yaw	65.1 m	75.4 m

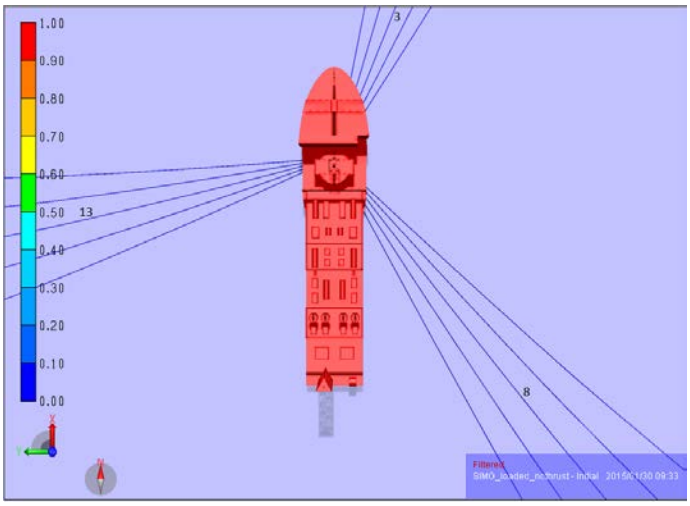

Figure 3 Vessel shown with mooring lines when the heading is towards north.

MODEL TESTS

The model tests were carried out in the 80 m × 50 m Ocean Basin at SINTEF Ocean in December 2016 and January 2017. The test programme was comprehensive, and included a number of tests with heading control. The purpose of the tests was partly design verification and partly to provide coefficients for mathematical modelling and simulation. The model scale was 1:60, see Figure 4. The FPSO's superstructure was modelled in detail to ensure accurate wind loads. In the basin, current can be generated in the basin's longitudinal direction. The basin has two wavemakers. One of these is a large double-flap that generates long-crested waves in the basin's longitudinal direction. The other consists of a large number of individual small wavemakers that are distributed along the long side of the basin. Within limits, this wavemaker can generate oblique waves and short-crested waves. Using this wavemaker, it is possible to make waves that are not co-linear with the current.

For the waves, the Torsethaugen sea spectrum [17] was used. The waves were long-crested. For wind gust, the spectrum according to ISO-19901-1 was used. The current was constant, apart from minor fluctuations.

METOCEAN ENVIRONMENT

Nine cases from the model test campaign were chosen for the study. Eight of the cases represent the FPSO in the loaded condition. Table 2 shows the metocean parameters of these tests. Four of the tests involve heading control. All cases include waves, wind and current. Note that the cases with and without heading control in Table 2 are not identical, as the directions differ.

The ninth case represents the ballasted condition and is a case of excitation by storm waves only (H_S = 12.9 m, T_p = 13.7 s). Without wind excitation, it is unrealistic. Still, the case is interesting for comparison of theory and reality (albeit down-scaled), because it represents a case of heading instability.

Figure 4 FPSO model (scale 1:60).

Table 2 Environment parameters of studied cases. *Hs* (m) is significant waveheight, *Tp* (s) is peak period, of wave spectrum, *Uwi* (m/s) is mean wind speed, and *Ucu (m/s)* is current speed. *Dir* (deg) denotes coming from directions.

	Case No.	ID	Wave			Wind		Current	
			H_s	T_p	*Dir*	U_{wi}	*Dir*	U_{cu}	*Dir*
No HC	1	4610	5.5	12.0	0	33	90	0.62	0
	2	4590	10.3	13.7	0	33	90	1.23	0
	3	4020	14.8	13.7	0	33	10	1.23	0
	4	4300	12.9	13.7	0	33	10	1.23	0
HC	5	4673	5.5	12.0	0	33	30	0.62	0
	6	4652	10.3	13.7	0	33	30	1.23	0
	7	4702	14.8	13.7	60	33	30	1.23	0
	8	4712	12.9	13.7	60	33	30	1.23	0

NUMERICAL MODEL

The computer program SIMO was used for the simulations. SIMO has a large repertoire of models and can handle multiple body systems. The FPSO is modelled with six degrees of freedom of motion. The wave frequency (WF) excitation forces are modelled by combining the excitation transfer functions from potential theory with the sea spectrum. The linear hydrodynamic reaction forces are modelled as retardation functions in combination with the infinite-frequency asymptote of added mass [4]. Wavedrift loads are computed using wavedrift coefficients, and slow-drift from waves are calculated by an improved version [10] of Newman's approximate method [15]. Loads from wind and current were modelled by direction dependent load coefficients determined from wind tunnel tests. Additional hydrodynamic damping, of viscous nature, is modelled by combinations of linear and quadratic force laws.

The mooring lines were modelled quasi-statically as combinations of catenaries relating tensions at the top ends to vessel position. As the software did not allow modelling of a vessel rotating about a turret, all mooring lines were attached to the turret centre. This models the turret as an ideal (frictionless) swivel.

In the simulations, one thruster of 1659 kN capacity and fixed sideways orientation replaces the three azimuth thrusters. The location of the thruster was chosen 117 m aft of midship (or 20 m forward of the AP). This was done to avoid issues relating to the quality of the thrust allocation. For heading control, the performance of the single, equivalent athwartship thruster can be regarded as the ultimate performance of the original azimuthing thrusters when high quality allocation is achieved.

The heading control system was modelled by SIMO's DP controller, which essentially is identical to the controller described in [16].

STABILITY ANALYSIS

Model in sway and yaw

The essential dynamic properties of the turret-moored FPSO can be investigated by linearizing the dynamic model about a state of static equilibrium. This enables calculation of the model's eigenvalues, which are the key to stability. We assume that only the horizontal components of motion need to be included in the model. Due to the 120˚ symmetry of the mooring system (Figure 3) the horizontal mooring stiffness is nearly independent of direction. Further, when studying the vessel's yaw behaviour and heading control, it is the interaction between yaw and sway that is most important. The restoring force of the turret mooring is sufficiently linear to rule out significant coupling from surge position to sway and yaw. Through nonlinear drag mechanisms, there will be some coupling from surge velocity to forces in sway and yaw. However, this effect is also believed to be weak and is therefore neglected (the assumption has not been checked, though). Hence, omitting surge from the model leaves a model in sway and yaw.

The sway-yaw model was derived from the full SIMO model by omitting all motion components, except sway and yaw, and removing the wave frequency parts. The zero frequency added mass was derived from the infinite-frequency added mass used by the extensive model (together with retardation functions).

Let $Y(\psi)$ be the static force in sway and $N(\psi)$ the static moment in yaw about the vessel centre. The moment about the turret centre then becomes

$$N_t(\psi) = N(\psi) - aY(\psi) \tag{1}$$

Here, a is the distance from the vessel centre to the turret centre. Let ψ_e *be* an equilibrium heading. Then

$$N_t(\psi_e) = 0 \tag{2}$$

Note that in general, the sway force at equilibrium will not be zero, i.e.

$$Y(\psi_e) \neq 0 \tag{3}$$

The sway-yaw model has the form

$$\begin{bmatrix} \boldsymbol{m} & \boldsymbol{0} \\ \boldsymbol{0} & \boldsymbol{mr^2} \end{bmatrix} \begin{bmatrix} \ddot{\boldsymbol{y}} \\ \ddot{\boldsymbol{\psi}} \end{bmatrix} + \begin{bmatrix} -\boldsymbol{Y_v} & \boldsymbol{0} \\ \boldsymbol{0} & -\boldsymbol{N_r} \end{bmatrix} \begin{bmatrix} \dot{\boldsymbol{y}} \\ \dot{\boldsymbol{\psi}} \end{bmatrix} + \begin{bmatrix} \boldsymbol{k} & \boldsymbol{ak - Y_\psi} \\ \boldsymbol{ak} & \boldsymbol{a^2k - N_\psi} \end{bmatrix} \begin{bmatrix} \boldsymbol{y} \\ \boldsymbol{\psi} \end{bmatrix} = \begin{bmatrix} \boldsymbol{Y} \\ \boldsymbol{N} \end{bmatrix} \tag{4}$$

where

- m - virtual mass in sway
- r - radius of gyration of yaw based on virtual mass in sway, m
- k - stiffness of turret mooring
- a - distance from vessel centre to centre of turret
- y - sway position of vessel centre of mass
- ψ - yaw angle
- Y_ψ - derivative of static environmental sway force with respect to yaw angle at equilibrium
- N_ψ - derivative of static environmental yaw moment with respect to yaw angle at equilibrium
- Y_v - derivative of sway force with respect to sway velocity at zero sway velocity.
- N_r - derivative of yaw moment with respect to yaw velocity, $r = d\psi/dt$, at zero yaw velocity (subscript r not to be confused with the radius of gyration)
- Y - External sway force, from metocean environment and thrusters
- N - External yaw moment about vessel centre, from metocean environment and thrusters

Note that the model expression Eq. (4) is simplified by setting $\psi_e = 0$, which means that the motion variables denote *deviations* from the equilibrium: ψ is the deviation from the equilibrium heading, and y is the deviation from the equilibrium sway position. In other words, $y = 0$ and $\psi = 0$ denote the equilibrium. Likewise, the loads Y and N become deviations from the static values.

The reference point for the sway motion is at the midship section, which is close to the centre of mass. Hence, there is negligible rigid-body inertia coupling between sway and yaw. Further, the effect of fore-aft asymmetry is no greater than justifying

that added mass and damping cross coupling can be neglected. Thus, the matrices of mass and damping become diagonal.

The spring stiffness of the turret mooring, on the contrary, gives strong coupling between sway and yaw, a coupling that characterises the dynamics of a turret-moored ship. The turret stiffness is almost independent of direction and constant over a large range of displacements. Hence, it is well represented by a single spring constant *k*.

The stiffness matrix in Eq. (4) is essentially and fundamentally non-diagonal. *The strongly coupled stiffness and weakly coupled mass and damping constitute the principal characteristic of a turret-moored vessel.*

For a discussion of the importance of various model parameters with respect to stability and robustness, see [14].

The model Eq. (4) is the result of linearization about a point of *static* equilibrium, which is the position and orientation at which the mooring forces - and possibly thruster forces - balance the static loads from the metocean environment. Static loads are the loads that act when the FPSO is at rest, i.e. 1) a constant current load corresponding to the constant current velocity, 2) a constant wind load corresponding to the mean wind velocity, and 3) the mean wavedrift force that corresponds to the wave spectrum and the direction of the waves.

The authors believe the formulation in Eq. (4) to express the essential dynamic properties of the turret-moored FPSO with regard to stability.

Eigenmodes

It is useful to study the eigenmodes to the sway-yaw model. An instructive insight in the system's characteristics is obtained by neglecting the damping and assuming no loading from the environment. In this case, Eq. (4) is reduced to a pure mass-spring system with symmetrical stiffness. It can be shown that the system with this simplification has the two eigenmodes shown in Figure 5, see [5]. One eigenmode is an unrestrained rotation about the turret centre. The other eigenmode is a pendular oscillation about a point aft of the centre. The authors of [11] have termed this mode the *metronome mode* by analogy with the mechanical metronome of the past. If a thruster acts through the pivot of the metronome mode (see Figure 5), it will control the first mode only. Likewise, a thruster acting through the turret centre will affect the metronome mode only. The thruster of the FPSO under study is located aft of the metronome mode's pivot. It will then act on both modes, but the effect on the metronome mode will be weak.

When we take the environmental loads and damping into the picture, the modes in the figure will be modified by the presence of the parameters Y_v, N_r, Y_ψ and N_ψ in Eq. (4), which depend on the environmental processes. The eigenmode representing rotation about the turret will be very sensitive to these, while the metronome mode is affected much less. This is demonstrated by the study [11], in which a large number of weather states, reconstructed by hindcasting over a period of fifty-six years, have been processed.

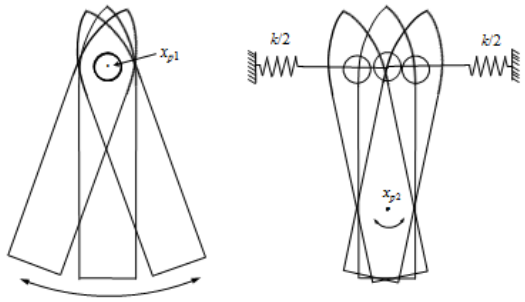

Figure 5 Illustration of the two sway-yaw pendulous modes of the undamped turret moored FPSO when no metocean loads are acting. Left: free rotation about a pivot at the turret centre. Right: oscillatory motion about a pivot aft of the vessel's centre of mass ('metronome mode'). The turret mooring is shown as lateral springs. The eigenfrequency of the mode is determined by the virtual mass in sway, the radius of gyration in yaw, the distance to the turret centre and the stiffness k of the turret mooring.

Criteria for stability

The criterion for stability is that all of the model's eigenvalues lie in the left half of the complex plane. The eigenvalues can be expressed as functions of the eight parameters in the model. Several authors have sought to express criteria for stability for the turret moored ship. The problem is analogous to that of determining straight-line stability of a sailing ship. The stability criteria of ship manoeuvring are also based on force derivatives like those in Eq. (4), often referred to as "hydrodynamic derivatives", see [1], [3]. The difference between a manoeuvring ship and a turret-moored ship is that the former has no mooring and that the latter has no constant forward speed.

Stability of a turret-moored ship has been investigated by a number of authors, [5], [7], [2], [18], [19], [20].

The eigenvalues to the sway-yaw model Eq. (4) are the roots of the model's characteristic polynomial, which is a polynomial of the fourth degree. While the solution for the roots on closed form exist, it is not practical to use. Conditions for stability can also be found from the coefficients of the characteristic polynomial using Routh's criterion [6], but the expressions become rather complicated [8] and give no insight or other advantage over numerically computed eigenvalues.

In the derivation of a simplified criterion for heading stability, we assume that the damping coefficients, $-Y_v$ and $-N_r$ of the sway-yaw model are positive. The damping will then be dissipative for any values of sway and yaw velocity. We then require that – with damping omitted – the remaining mass-spring model be a conservative system. This means that any inherent mechanical energy will remain constant as long as there is no excitation. With damping included, the inherent energy will die out, and the

system is consequently stable. We therefore heuristically consider the conservatism of the mass-spring model as a *sufficient* criterion for stability. Conservatism of the damping-free system is ensured by requiring all the eigenvalues to be purely imaginary. This gives the following three conditions for stability:

$$k(a^2 + r^2) > N_\psi \qquad (i)$$

$$aY_\psi > N_\psi \qquad (ii) \qquad (5)$$

$$\frac{\left[N_\psi + k(r^2 - a^2)\right]^2}{4akr^2} + ak > Y_\psi \qquad (iii)$$

For a given FPSO, loading condition and turret mooring, the parameters a, k and r are fixed, while Y_ψ and N_ψ depend on the environmental conditions. It is noted that inequality (*ii*) above states that the slope of the moment about the turret must be negative at the equilibrium heading, cf. Eq. (1). This is sometimes referred to as the static stability criterion, as it does not involve parameters that govern the system's dynamic behaviour, i.e. mass and mooring stiffness.

Before turret mooring came into use, stability of vessels with single point mooring was studied, and resulted in conditions similar to those above, see [13].

Stability of cases without heading control

For the freely weathervaning cases in Table 2 (i.e. cases 1 – 4), the pairs of the parameters Y_ψ and N_ψ are calculated and shown in Figure 6 together with lines indicating the stability conditions according to Eq. (5). The stability is computed for the headings of equilibrium. From the figure, we see that Case 2 is unstable, violating condition *iii*. Case 3 lies on the stability limit.

Figure 7 shows the eigenvalues of the same cases as points in the complex plane. The sway-yaw model has four eigenvalues that may occur as points on the real axis or in complex conjugate pairs. For the four cases shown in the figure, all eigenvalues are complex. The points closest to the imaginary axis represent the 'metronome mode' in Figure 5, or rather this mode as it is modified by the parameters Y_ψ and N_ψ. All eigenvalues are located in the left half plane. The model is consequently stable. This shows that when damping is taken into account, cases that are deemed unstable by the sufficiency criterion Eq. (5) can be stable after all. The figure shows that the eigenvalues of the metronome mode are located rather close to the imaginary axis. This means that they are lightly damped and represent modes of oscillatory character.

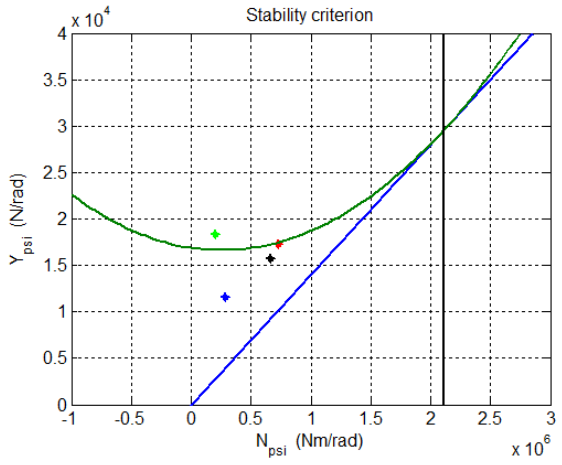

Figure 6 Pairs of parameters Y_ψ and N_ψ for cases 1 (blue), 2 (green), 3 (red), 4 (black). No heading control. The three lines show the three stability limits given by Eq. (5). For stability, the points must lie to the left of the black line (5 *i*), above the blue line (5 *ii*) and below the green line (5 *iii*).

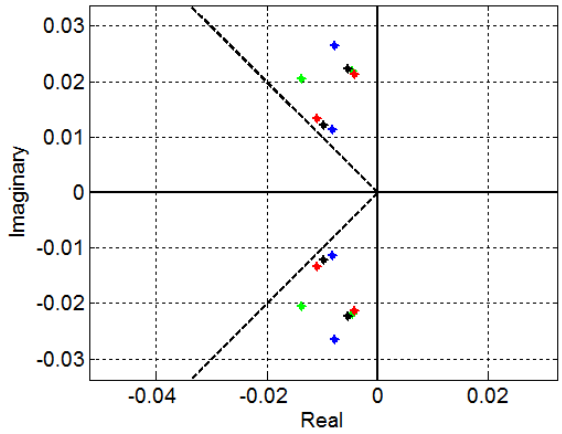

Figure 7 Eigenvalues of cases 1 (blue), 2 (green), 3 (red), 4 (black). Without heading control. The dashed lines indicate a damping ratio of 0.7.

Heading Control

When a heading different from the natural weathervaning heading is wanted, the use of thrusters is necessary for generating the required moment of force to maintain the heading. This can be obtained by a heading control system doing *integral control*. In this case, the required moment is calculated automatically by the control system. However, a forced heading may not be a stable heading, or it may have poor stability. In this case, additional moment stiffness about the turret is required. This can be obtained by adding proportional control. Finally, derivative control may be required to damp oscillations. The controller then becomes a PID controller, which is the most common controller for SISO (single input, single output) systems, i.e. systems that have one control input and one response output, like heading control with a single thruster:

$$Y_{thr} = -g_P\psi - g_V\dot{\psi} - g_I \int \psi \, dt \qquad (6)$$

Here, Y_{thr} is the force from the thruster, ψ the heading error, and g_P, g_V and g_I the controller gains of proportional, derivative (velocity) and integral feedback. The moment from the thruster (about the FPSO centre) is

$$N_{thr} = a_{thr}\, Y_{thr} \qquad (7)$$

where a_{thr} = -117 m is the longitudinal location of the thruster. The proportional gain was chosen as:

$$g_P = -100 \cdot a_{thr} = 11700 \text{ kN/rad} \qquad (8)$$

The number 100 (kN/m) is comparable to the stiffness of a local lateral spring acting at the location of the thruster. For comparison, the stiffness of the turret mooring is 233 kN/m (An important difference from a real spring is that the artificial rear spring only acts on local displacements caused by heading deviations). The derivative gain (velocity gain), g_V, was chosen such that it gave a damping ratio of 0.6. The integral gain was given a value small enough not to interfere with the controller's stability, yet not so small it would cause impractically long settling times in tests and simulations.

When we incorporate the gains of the controller in the sway-yaw model, the stability criterion in Eq. (5) gives the result shown in Figure 8. All the four cases are now in the unstable region. Hence, it seems that the controller has worsened the situation. However, as pointed out above, the conditions of the criterion are not conditions of necessity. Taking damping into the calculation and computing eigenvalues, gives the result in Figure 9. Now, all eigenvalues are stable. Comparing with the weathervaning case in Figure 7, we see that the 'non-metronomic' eigenvalues have moved towards the left. All of these eigenvalues lie to the left of the dashed lines, which shows that the corresponding modes are damped rapidly. In fact, the damping is stronger than necessary. It can be shown that in this case only integral control would be sufficient.

Comparing Figure 7 and Figure 9, we also see that the controller has not influenced the eigenvalues of the metronome mode much, as expected.

SIMULATION AND MODEL TESTS

The eight cases in Table 2 were simulated with SIMO, using the full model with six degrees of freedom of motion. SIMO has a more sophisticated DP controller than the simple PID described above; in that the controller also uses a state observer of Kalman filter type, including adaptive wave filtering, see [16]. Still, the controller essentially is a PID controller. The controller gains were chosen equal to those used in the eigenvalue analysis above.

Table 3 shows statistics from the simulations. For the cases without heading control, the mean headings compare well. This shows that the load coefficients of current and wind are realistically rendered by the wind tunnel tests. In addition, the wave-drift coefficients obtained from potential theory seem to be realistic.

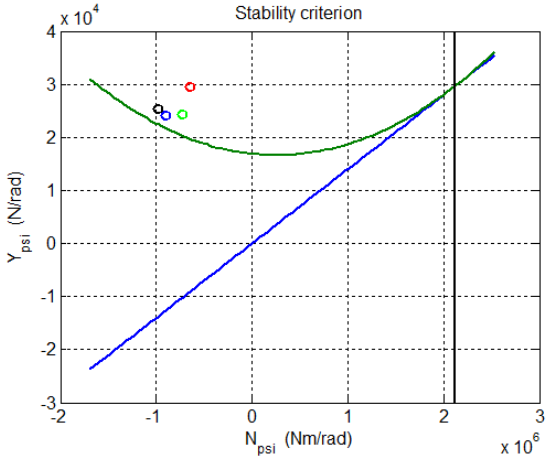

Figure 8 Stability criterion with heading control. Case 5 (blue), Case 6 (green), Case 7 (red), Case 8 (black).

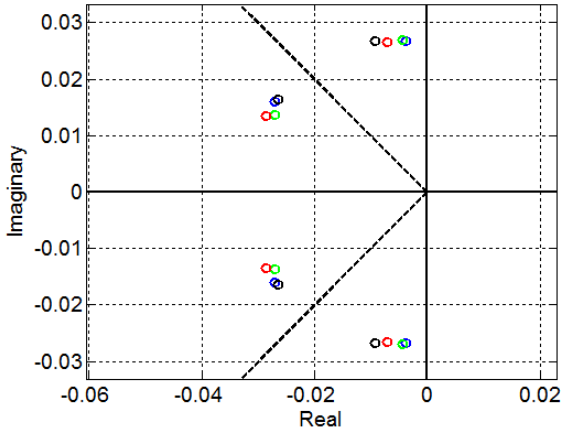

Figure 9 Eigenvalues with heading control and bow against the waves. Cases: 5 (blue), 6 (green), 7 (red), 8 (black). The dashed lines indicate a damping ratio of 0.7.

The standard deviations match less well. Still, all the four cases are stable, as indicated by the eigenvalues in Figure 7.

The magnitude of the dynamic heading is strongly dependent on the damping in yaw. Apart from some adjustment of the yaw damping, no tuning of the numerical model has been carried out. With more careful tuning better agreement is expected.

For Case 2, the time histories of heading from experiment and simulation are shown in Figure 10. The time histories are reasonably similar, but the simulated heading appears to have somewhat more slow variation. Figure 11 shows power spectra. Both the test and the simulation show two distinct peaks. The peak on the right correspond reasonably well to the metronome mode; the other peak is not readily explained.

For the cases with heading control, i.e. cases 5 - 8 in Table 2, the mean values from test and simulation compare well. For cases 7 and 8 the mean value ought to be 60 degrees, but are slightly less due to occasional thruster saturation. Both the experiments and the simulations reflect this phenomenon.

The standard deviations from the simulations are smaller than those of the model tests. Although the controller gains in experiments and simulations are similar, the controllers are not perfectly identical: The signal filtering is different, and there is always more error sources in real life.

Time traces and spectra for Case 6 are shown in Figure 12 and Figure 13, respectively. Apart from the difference in magnitude, the spectra essentially have the same shape. The resonant behaviour of the metronome mode is clearly seen. However, the frequencies of the spectral peaks of the simulations and the experiments differ significantly. This is difficult to explain. The spectral peak from the simulation occurs at about 0.0037 Hz = 0.023 rad/s. According to the eigenvalues in Figure 9, the resonant frequency is about 0.027 rad/s.

Comparing with the non-controlled case in Figure 11 (although these cases do not represent identical environments) we see that the energy below 0.003 Hz has been eliminated. This shows that the controller is effective, both in the simulations and in the model tests.

Table 3 Mean value and standard deviation of heading.

	Case No.	ID	Model test		Simulation	
			Mean	St. dev.	Mean	St. dev.
Without heading control	1	4610	60.5˚	5.2˚	55.7˚	4.2˚
	2	4590	48.5˚	5.0˚	41.8˚	5.7˚
	3	4020	9.1˚	3.6˚	9.7˚	3.4˚
	4	4300	7.9˚	3.9˚	9.8˚	2.6˚
With heading control	5	4673	0.0˚	3.1˚	0.0˚	1.8˚
	6	4652	0.0˚	2.5˚	0.1˚	1.9˚
	7	4702	57.9˚	2.6˚	59.0˚	1.9˚
	8	4712	57.8˚	2.8˚	59.0˚	1.8˚

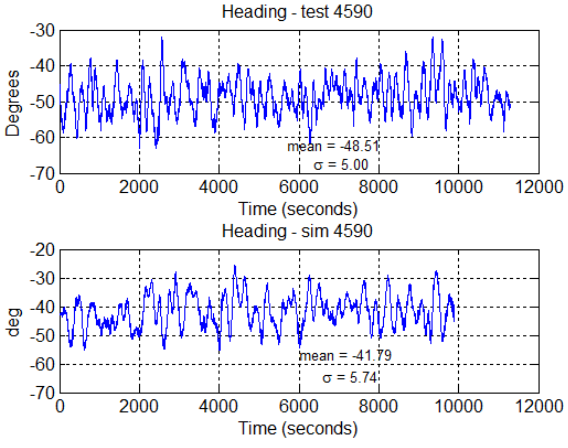

Figure 10 Heading from test and simulation. No heading control. Case 2 in Table 2 and Table 3.

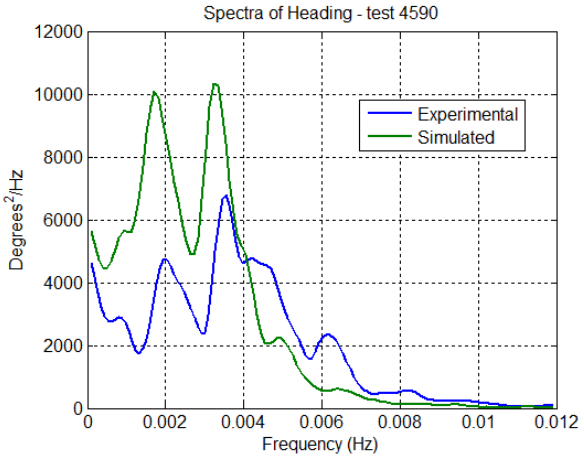

Figure 11 Power spectra of heading from experiment and simulation. No heading control. Case 2 in Table 2 and Table 3.

A case of instability – ballasted ship

Above, it was found that the loaded FPSO was stable in all the eight investigated cases. To study a case of instability, a ninth case was found among the model tests. This test was done with the ballasted ship. It involved excitation from waves only, attacking at an angle of 60 degrees. The significant wave height and peak period were 12.9 metres and 13.7 seconds, respectively. Consequently, the case is not likely to happen in reality.

Figure 14 shows the heading from the model test and a simulation carried out with a model for the ballasted condition. Although different, both the experiment and the simulation clearly show an unstable or poorly stable situation.

Figure 15 shows the wavedrift moment about the turret (in blue) as function of vessel heading. The curve indicates stability at sixty degrees (cf. expression *ii* in Eq. (5), although the negative slope of the curve at the zero crossing is small. For comparison, the turret moment corresponding to a *Jonswap* sea spectrum with

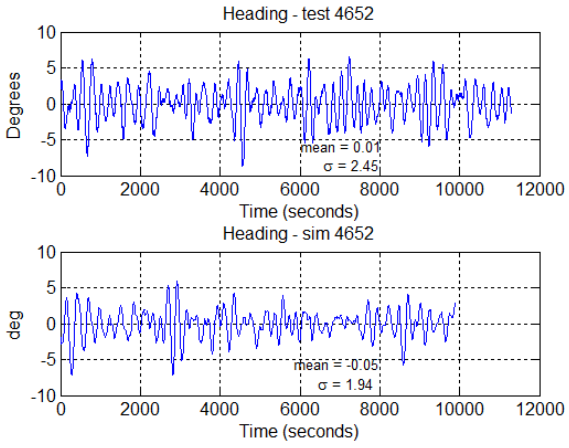

Figure 12 Heading from test and simulation. With heading control.

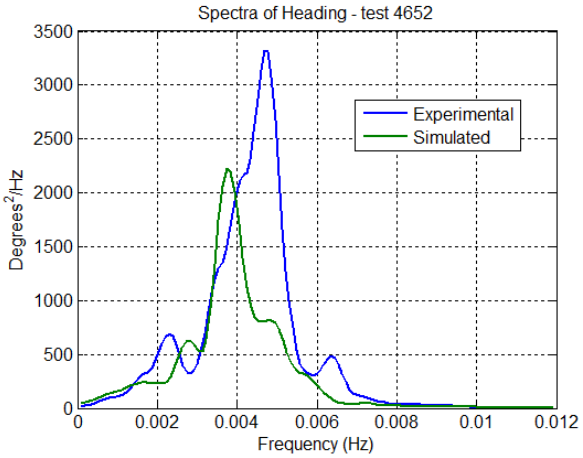

Figure 13 Power spectra of heading from experiment and simulation. With heading control. Case 6 in Table 2 and Table 3.

γ = 3.3 is shown. According to the latter curve, the heading 60 degrees is not stable. Instead, there are two stable points at 45 and 75 degrees (bifurcation).

The simplified stability criterion in Figure 16 shows that both wave spectra result in (N_ψ, Y_ψ) -points lying close to the stability limit. However, with the Torsethaugen spectrum the system is barely stable, while it is just unstable with the Jonswap spectrum. For identical significant wave height and peak period and a gamma value of 3.3 for the Jonswap spectrum, the Jonswap spectrum is somewhat narrower than the Torsethaugen spectrum. This shows that the behaviour of the vessel can be sensitive to the shape of the sea spectrum.

Between 2000 and 4000 seconds in the simulated time history in Figure 14 the heading seems to be stable around 60 degrees. This is probably the effect of the low, but positive restoring stiffness in Figure 15, as long as the disturbance from the waves is small. When larger disturbance happens, the heading is easily driven away from the point of equilibrium. This is in contrast to the test in the upper plot, which seems not to have a point of equilibrium.

CONCLUSION

A turret-moored FPSO with a heading control system is studied to learn about its expected heading response in storm conditions. It has been of particular interest to investigate the conditions for heading stability and see if simple criteria derived from the linear model in sway and yaw, can give useful information about the stability.

It is known that the motion characteristics of a turret-moored ship are sensitive to the magnitude of the metocean parameters, and of the spreading of the directions of waves, wind and current. For the study, cases from model tests are chosen, some with, some without heading control.

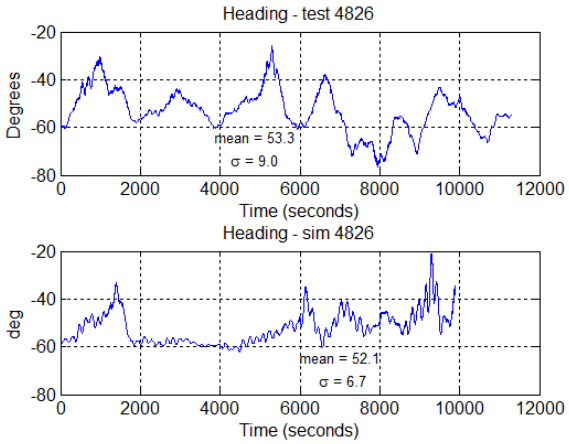

Figure 14 Heading from model test (upper) and simulation showing poor heading stability. Ballasted condition.

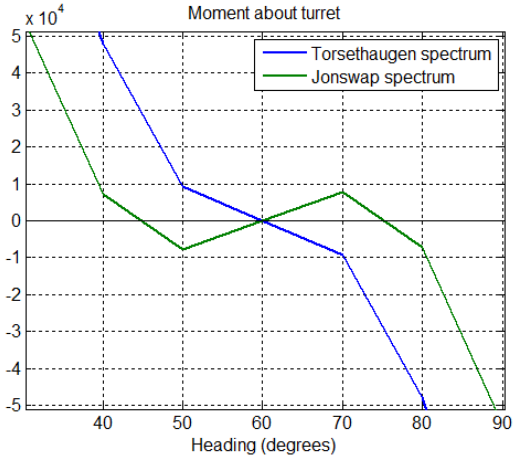

Figure 15 Wavedrift moment about turret, dependent on spectrum type. Ballasted condition (The resolution of the load curves is 10 degrees).

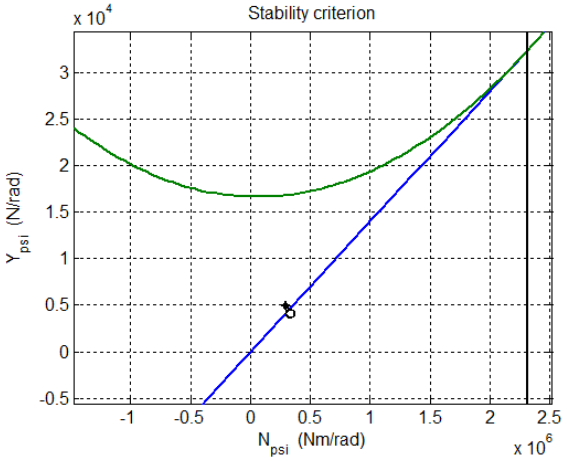

Figure 16 Stability depending on type of sea spectrum. Asterisk: Torsethaugen spectrum, Circle: Jonswap spectrum.

A simple stability criterion is formulated. It consists of three conditions depending on the derivatives of sway force and yaw moment with respect to heading angle. The criterion uses no damping information and is assumed to be a sufficiency criterion for heading stability.

A more comprehensive criterion uses the eigenvalues of the linearized sway-yaw model. This is a numerical criterion.

A full SIMO model with six degrees of freedom of motion is established for the FPSO.

According to the simple criterion, all but one case without heading control are stable, while all cases with control are unstable. The eigenvalues indicate stability for all the eight cases. Both the experiments and the simulations with SIMO confirm this. Hence, the sufficiency property of the simplified criterion is not contradicted. However, the criterion appears to be rather conservative, at least when the neglected damping is significant. In one additional example with hypothetical excitation from storm waves only, the simplified criterion agrees well with simulation and experiment.

The heading controller used in the study is of simple SISO PID type, but manages to reduce the FPSO's yaw response significantly.

ACKNOWLEDGEMENTS

The authors thank Statoil for the permission to publish the material described herein. We also thank Mette Grahl-Nielsen and her colleagues at Aker Solutions for supplying data for the simulation model.

REFERENCES

[1] Abkowitz, M. A., "Lectures on Ship Hydrodynamics – Steering and Manoeuvrability", Report No. Hy-5, Hydro and Aerodynamics Laboratory, Lyngby, Denmark, 1964.

[2] Bernitsas, M. M., Garza-Rios, L. O., Kim, B.-K., " Mooring Design Based on Catastrophes of Slow Dynamics", Report No. 340, Department of Naval Architecture and Marine Engineering, University of Michigan, Ann Arbor, MI, USA, 1999.

[3] Comstock, J. P. (ed.), "Principles of Naval Architecture", Society of Naval Architects & Marine Engineers, New York, N. Y., USA, 1967

[4] Cummins, W. E., "The Impulse Response Function and Ship Motions", Report, David Taylor Model Basin, Washington DC, USA, Oct. 1962

[5] O'Donoghue, T. and Linfoot, B. T., "Performance of Turret-Moored Systems in Waves", Proceedings of the 1st International Offshore and Polar Engineering Conference, Edinburgh, United Kingdom, 11-16 August 1991.

[6] Franklin, G. F., Powell, J. D., and Emami-Naeini, A, "Feedback Control of Dynamic Systems", 7th ed., Pearson Education Ltd, London, UK, 2015

[7] Garza-Rios, L. O. and Bernitsas, M. M., "Slow motion dynamics of turret mooring and its approximation as single point mooring", Applied Ocean Research 21, 1999

[8] Garza-Rios, L. O. and Bernitsas, M. M., "Analytical Expressions of the Stability and Bifurcation Boundaries for General Spread Mooring Systems", J. of Ship Research, Vol. 40, No. 4, Dec. 1996, pp 337-350.

[9] Howell, G. B., Duggal, A. S., Heyl, C., Ihonde, O., "Spread Moored or Turret Moored FPSO's for Deepwater Field Developments", Offshore West Africa, Abuja, Nigeria, 2006.

[10] Kaasen, K. E., "An Improvement to Newman's Method for Approximate Calculation of Slow-Drift Wave Force Eliminating the high Frequency Noise", OMAE1999, St. John's, Canada, 1999

[11] Kaasen, K. E, Ludvigsen, H. and Aas K., "Heading Control of a Turret-Moored FPSO With and Without Forward Thrusters. Paper OTC-27794, Offshore Technology Conference, Houston, Texas, USA, 1-4 May 2017

[12] Kaster, F., Barros, M., Rossi, R., Masetti, I., Falkenberg, E., Karlsen, S., Waclawek I., "DICAS – A New Mooring Concept for FPSO's", OTC-8439-MS, Offshore Technology Conference, Houston, Texas, USA, 1997.

[13] Liapis, N., "Wave Loads and Motion Stability of a System of Rigid Bodies", Doctoral thesis, Div. of Marine Hydrodynamics, NTH, Trondheim, Norway, 1979

[14] Matsuura, J. P. J., Bernitsas, M. M., Garza-Rios, L. O. and Nishimoto, K., "Sensitivity and Robustness of Hydrodynamic Mooring Models", Proceedings of the 20th International Conference on Offshore Mechanics and Arctic Engineering (OMAE2001/OFT-1300), Rio de Janeiro, Brazil, June 3-8, 2001.

[15] Newman, J. N., “Second-order, Slowly-varying Forces on Vessels in Irregular Waves”, Paper 19, Int. Symposium on the Dynamics of Marine Vehicles and Structures in Waves, University College, London, 1974

[16] Sælid S, Jenssen N A, Balchen J. G., "Design and analysis of a dynamic positioning system based on Kalman filtering and optimal control", IEEE Transactions on Automatic Control, 28 (3) : 331-339, 1983 .

[17] Torsethaugen, K., "Simplified double peak spectral model for ocean waves", Report STF80 A048052, SINTEF Fisheries and Aquaculture, Trondheim, Norway, 2004

[18] Zangeneh, R. and Thiagarajan, K. P., "Heading Stability Analysis of FPSOs", Proceedings of the Twenty-fifth International Ocean and Polar Engineering Conference", Kona, Big Island, Hawaii, USA, June 21-26, 2015

[19] Zangeneh, R., Thiagarajan, K. P., Urbina, P. and Tian, Z., Effect of viscous damping on the heading stability of turret-moored tankers", Ships and Offshore Structures, 2016, DOI: 10.1080/17445302.2016.1165554

[20] Zangeneh, R., Thiagarajan, K. P., Cameron, M., "Effect of Wind Loads and Damping on Heading Stability of FPSOs", Proceedings of the 36th International Conference on Ocean, Offshore and Arctic Engineering (OMAE2017), Trondheim, Norway, June 25-30 2017.

